Water in Celtic Countries: Quantity, Quality and Climate Variability (Proceedings of the Fourth InterCeltic Colloquium on Hydrology and Management of Water Resources, Guimarães, Portugal, July 2005).
IAHS Publ. 310, 2007.

Application of Artificial Neural Networks for river flow simulation in three French catchments

MONOMOY GOSWAMI & KIERAN M. O'CONNOR

Department of Engineering Hydrology, National University of Ireland, Galway, Ireland
monomoy.goswami@nuigalway.ie

Abstract For more than a decade, Artificial Neural Networks (ANNs) have been increasingly used in hydrology as flexible black-box models of non-linear type. Within this category of models, the "multi-layer feed-forward network" used in this study consists of an input layer, an output layer, and one "hidden" layer in between. The model is applied to daily data of three catchments, all located in northwest France, for river flow simulation and forecasting and its performance is compared with those of five system-theoretic models and one conceptual model. The ANN is observed to be the best performing individual model for the catchments tested. In the subsequent application of the Neural Network Method (NNM) for combining the outputs of the individual models, in different combinations, i.e. in a "multi-model approach" for deriving consensus forecasts, the NNM (as one of three Model Output Combination Techniques (MOCTs) considered) is found to be the best performing MOCT and also better than the best individual model. The Galway Flow Modelling and Forecasting System (GFMFS), a software package developed by the present authors, is used in the study.

Key words black-box models; hidden layer; multi-model approach; Neural Networks

INTRODUCTION

With the advent of advanced computing technologies, newer concepts and techniques such as Artificial Neural Networks (ANNs) have found extensive use in hydrology. ANNs, being conceptually analogous to the biological neural network controlling the functions of the human brain, are highly interconnected networks of basic processing units, called neurons, and have weights associated with the links (or information pathways) between the neurons. The ANN approach is essentially data driven and considered to be appropriate in situations where the overall transformation process and its sub-processes are not explicitly defined, and satisfactory explanations of the physical relationships involved can not be advanced. As deep physical interpretations cannot be ascribed to the weights determined during training of the ANNs (Minns & Hall, 1996), the models based on ANNs are considered as being "black-box", of non-linear type. For simulating and forecasting river flows, the outputs of the highly non-linear, complex, and dynamic rainfall–runoff transformation process, ANNs have been successfully applied as efficient tools. Many studies have been carried out on the data of different catchment types for improving the performance of rainfall–runoff transformation models by using different network architectures, learning rules and training algorithms (e.g. Halff *et al.*, 1993; Smith & Eli, 1995; Shamseldin, 1997;

Dawson & Wilby, 1998; Campolo *et al*., 1999; Tokar & Johnson, 1999; Zealand *et al*., 1999; Birikundavyi *et al*., 2000; Tingsanchali & Gautam, 2000; Sivakumar *et al*., 2002; Jain & Indurthy, 2003; Rajurkar *et al*., 2004). Innovative ANN applications include those of Hu *et al*. (2001) who developed the "range dependent" neural networks based on the clustering algorithm, Shamseldin *et al*. (1997) and Shamseldin & O'Connor (1999, 2001) who used ANNs for combining outputs of individual models and for forecast updating, and Toth *et al*. (2000) who applied ANNs to predict short-term rainfall for real time flood forecasting.

In the present study, a multiple-input single-output feed-forward form of neural network is used for continuous rainfall–runoff simulation, operating firstly as an individual model (ANN) and subsequently as a method (NNM) for combining the outputs from a number of different individual substantive models, including the ANN. Three catchments, located in the northwest of France, have been chosen for the study. The performance of the ANN as an individual model is compared with that of the conceptual Soil Moisture Accounting and Routing model with Groundwater modification (SMARG), two forms (parametric P and non-parametric NP) of two system-theoretic models, namely, the naïve Simple Linear Model (P-SLM and NP-SLM) and the quasi-linear seasonally-based Linear Perturbation Model (P-LPM and NP-LPM), and finally the wetness-index based system-theoretic Linearly-Varying Gain Factor Model (LVGFM). In each case, model simulation performance is evaluated on the basis of the Nash-Sutcliffe R^2 index of model efficiency (Nash & Sutcliffe, 1970).

As a separate exercise, following the multi-model approach for simulating the flows by combining outputs from different models, three Model Output Combination Techniques (MOCT) are applied in which strengths of individual models are pooled and perceptible weaknesses de-emphasized, producing a "consensus" forecast. The selected MOCTs are the Neural Network Method (NNM), the Weighted Average Method (WAM), and the Simple Average Method (SAM, as a naïve form of MOCT). The simulation performances (R^2) of the MOCTs as well as the performance of the MOCTs vis-à-vis the best of the individual models are compared to assess the efficacy of the MOCT concept for the test catchments. On the basis of the results, conclusions are drawn and recommendations made.

THE CATCHMENTS AND THE DATA CHARACTERISTICS

The three small catchments considered in the study, identified here simply by their station codes J2034010, J3024010, and J4124420, are located in Bretagne (Brittany) province in northwest France. Daily data for these catchments were generously provided by Météo France and the Direction de l'Eau for application in the MOPEX (Model Parameter Estimation Experiment) Project, and made available to the present authors for their contribution to the July 2004 MOPEX Workshop held in Paris. Table 1 provides some salient features of the catchments, and their locations are shown in Fig. 1. As seen in Table 1, all three catchments have practically the same mean catchment altitude, their mean slopes being flatter than 1 in 100, and their areas (all small) are of the same order of magnitude.

Summary characteristics of the daily hydrological data for the catchments are given in Table 2. The seasonal mean variations of evaporation, rainfall and discharge, all smoothed by Fourier harmonic analysis (using four harmonics), are shown in Fig. 2. Each data set has 2557 data points (for seven years), starting from 1 August 1995. The hydrological characteristics of all three catchments display considerable uniformity in values and distribution throughout the data period which suggests that all three belong to the same hydrological regime. For J4124420, the flow generation is least, and the evaporation highest.

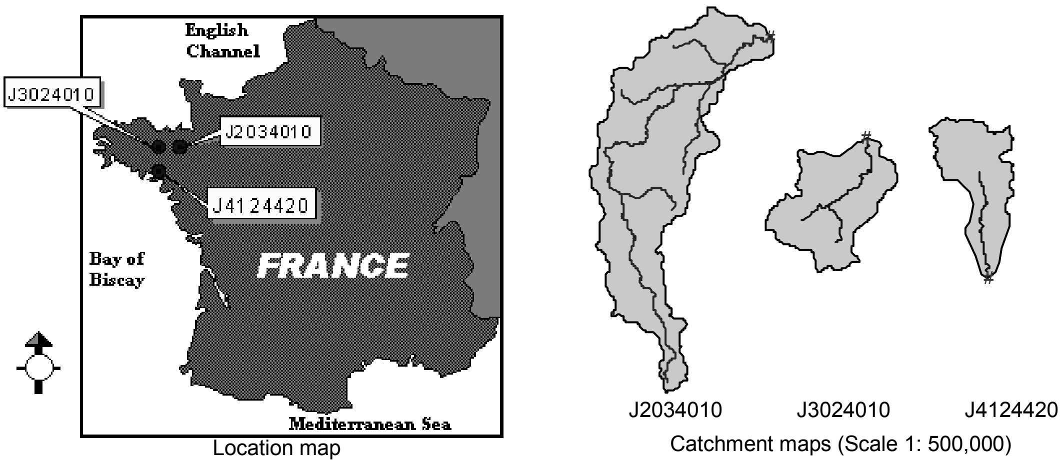

Fig. 1 Location map along with shape and size of the three catchments.

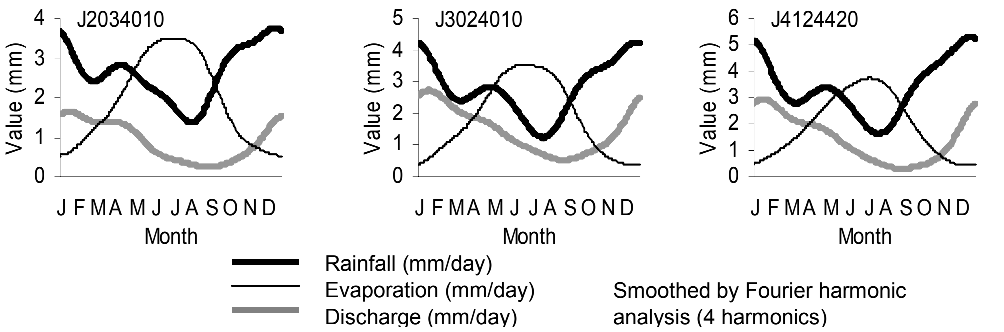

Fig. 2 Smoothed seasonal variation of the hydrological variables.

Table 1 Catchment characteristics.

Station Code No.	Station Name	Area (km^2)	Length of longest stream (km)	Altitude at outlet (m)	Altitude at highest point (m)	Mean altitude (m)
J2034010	Le Guindy à Plouguiel	125	42.1	20	300	83
J3024010	Le Guillec à Trézilidé	43	11.6	35	120	85
J4124420	La Rivière de Pont-l'Abbé à Plonéour-Lanvern [Tremillec]	32.1	9.0	15	158	84

MODELS AND EFFICIENCY CRITERIA

With the exception of the naïve SLMs (NP-SLM and P-SLM, used purely as base-line models), all the individual models applied in this study, namely, the conceptual SMARG model, the Linear Perturbation Model (P-LPM and NP-LPM), and the Linearly-Varying Gain Factor Model (LVGFM) were developed at the Department of Engineering Hydrology at the National University of Ireland, Galway, Ireland.

Table 2 Characteristics of hydrological daily data (period 1 August 1995–31 July 2002).

Catchment	Discharge Q (mm day^{-1})				Rainfall R (mm day^{-1})				Evaporation E (mm day^{-1})				%
	Max	Min	Mean	SD	Max	Min	Mean	SD	Max	Min	Mean	SD	days $R>E$
J2034010	11.8	0.10	0.89	0.90	45.8	0.0	2.63	4.56	3.7	0.50	1.94	1.11	37.3
J3024010	14.4	0.30	1.45	1.28	49.9	0.0	2.78	4.66	3.6	0.34	1.88	1.17	38.7
J4124420	8.94	0.08	1.43	1.43	55.5	0.0	3.38	5.96	4.4	0.48	1.97	1.20	38.1

The "Galway Flow Modelling and Forecasting System (GFMFS)", a software package incorporating a suite of different hydrological models and techniques, also developed in Galway by the present authors, was used. These models are described elsewhere (e.g. Kachroo & Liang, (1992), for SLM and LPM; Ahsan & O'Connor, (1994), for the LVGFM; Kachroo, (1992), for SMAR, the original version of SMARG; Goswami *et. al.* (2002) for SMARG and comprehensive description of all models used in this study). Likewise, the three MOCTs (SAM, WAM, and NNM) are described by Shamseldin *et al*. (1997). Note that the structure of the individual ANN rainfall–runoff model is identical to that of the NNM form of MOCT used for consensus forecasting of flows. For each neuron in the hidden layer (and also that in the output layer) of the neural networks used in this study, the received input array y_i is transformed to its output y_{out} by the non-linear S-shaped activation transfer function:

$$y_{out} = f\left[\sum (w_i y_i + w_o)\right] = 1 \Big/ \left[1 + \exp\left\{-\sigma \sum (w_i y_i + w_0)\right\}\right] \tag{1}$$

where $f(\,)$ denotes the transfer function, w_i is the input connection pathway weight, the summation extends from $i = 1$ to $i = M$, the total number of inputs, and w_o is the neuron threshold (or bias), i.e. a base-line value independent of the input. The term on the right hand side of Equation (1) is the widely-used logistic function, a form of sigmoid function, bounded in the range [0,1]. The weights w_i, the threshold (or bias) w_0 and the σ of different neurons can be interpreted as parameters of the selected network. If "L" is the total number of neurons in the input layer and "m" is the total number of neurons in the hidden layer, then the total number of weights to be estimated for the ANN or NNM models, is $[(L+1)m + (m+1)]$.

Despite its well-known shortcomings (Kachroo & Natale, 1992), only the dimensionless global model-output efficiency index R^2 (Nash & Sutcliffe, 1970) is used in this paper for judging the relative performance of the individual models and the MOCTs. Whereas $R^2 = 1$ would denote the ideal or "perfect" fit, it is generally agreed that $R^2 > 90\%$ is indicative of a very good model fit, while that in the range of 80–90% is a fairly good fit, and a range of 60–80% is considered unsatisfactory.

METHODOLOGY

Data gaps in the discharge series for J4124420 were synthetically filled by: (i) initially assuming –9.99 as the data value for each missing number, and (ii) calibrating each model iteratively until the model performance in two successive tests converged, the discharge series used for filling the gaps in each iteration being the corresponding discharge estimates of the data values simulated in the previous iteration. For each model, the series having the best (i.e. highest) R^2 performance value was adopted for filling the original gaps in the series.

For the NP-SLM, the NP-LPM, and the LVGFM, the ordinary least squares (OLS) method is used for estimation of the system response function. Calibration for these models involves determining a suitable value of memory length by trial and error by noting each time the shape of the system response until a satisfactory shape is obtained for a particular value of the memory length and near-maximum value of R^2. The OLS procedure is adopted also for estimation of parameters of the P-SLM and the P-LPM. For the SMARG model, the optimum parameter set is optimized using the Simplex search method by varying the memory length (by trial and error) of the surface runoff response function, and also the starting values and bounds of the parameters.

The connection pathway weights (w_i) and the different neuron threshold values (w_0) for the ANN model are estimated by a procedure usually referred to as training (or simply as calibration). Rather than the more commonly used back-propagation learning algorithm, the Simplex optimization procedure is used in the present study in searching for the "optimum" parameter set i.e. the "best" values of the connection weights. For the input and hidden layers, the number of neurons required for achieving the near-maximum value of R^2 was selected by trial and error.

The SAM, WAM, and NNM forms of MOCT were applied to the outputs of all seven individual models, together with those of the best 6, 5, 4, 3, and finally the best 2 models.

The "split-record evaluation procedure" was adopted for calibration and validation of all models. Whereas data starting from the first data point to the end of the fourth year were used for calibration, the R^2 values were evaluated over the last three calibration years, considering the first water-year's data as the "warm-up" period. This warm-up period is in conformity with that adopted for all catchments, including the three catchments considered in the present study, at the Paris MOPEX Workshop of 2004 (O'Connor *et al*., 2004). The relative performance of the models is adjudged from the R^2 values in calibration.

RESULTS AND DISCUSSIONS

Table 3 shows the R^2 values for each of the three catchments obtained by running each calibrated model. Because of the naïve SLM representation of the outflow series as simply the convolution summation of the response function with the inflow series, the performances of the P-SLM and the NP-SLM are, as expected, generally inferior to those of all other models, with the unconstrained NP-SLM form being generally better than that of the constrained P-SLM.

Table 3 R^2 values in calibration (R_c^2) and verification (R_v^2) produced by seven models, and ranks.

Model	J2034010			J3024010			J4124420		
	R_c^2	R_v^2	Rank	R_c^2	R_v^2	Rank	R_c^2	R_v^2	Rank
P-SLM	47.75	54.42	7	31.44	37.29	7	50.89	54.66	7
NP-SLM	48.00	55.66	6	46.72	52.62	6	52.51	57.95	6
P-LPM	73.64	60.30	5	69.47	47.43	5	75.46	52.84	5
NP-LPM	75.70	69.19	4	70.11	53.98	4	82.90	73.34	3
SMARG	81.64	81.46	3	85.85	78.17	3	80.50	89.10	4
LVGFM	85.65	92.14	2	86.61	88.48	2	86.54	87.42	2
ANN	**91.87**	**89.51**	**1**	**90.32**	**86.87**	**1**	**90.38**	**89.19**	**1**

As a result of the seasonality exhibited by the rainfall and the discharge series (see Fig. 2), the performances of the P-LPM and the NP-LPM are significantly better than their SLM counterparts. For the catchments J2034010 and J3024010, a significantly better fit of the simulated discharge series is obtained by the conceptual SMARG model (in comparison with these four system-theoretic models), the R^2 value with the SMARG model being more than 80% in both cases for both calibration and verification. However, for J4124420, the R^2 value obtained by SMARG model, while still greater than 80%, is nevertheless slightly lower than that produced by the NP-LPM for the calibration period but significantly higher for the validation period. The LVGFM, an elaboration of the NP-SLM that uses the output of the best amongst the five above-mentioned models (SMARG, for all three catchments) as an auxiliary model to introduce linear variation of the gain factor with the selected catchment wetness index at each time-step, performs better than both forms of the SLM and the LPM, and its auxiliary model, SMARG. However, the ANN model, which uses the recent outputs from the best stand-alone model (SMARG) as inputs to the neurons in the input layer (in order to simulate storage effects) along with recent rainfall inputs, performs better than the LVGFM, the SMARG, and both forms of the SLM and LPM models. The ANN model, therefore, performs best among the individual substantive models tested, for all three catchments. The type of input series and the number of previous observed data values for the neurons in the input layer, the number of neurons in the hidden layer, and the resulting number of weights optimized for the chosen ANN models are provided in Table 4. Although the number of weights (i.e. parameters) for describing the network renders the ANN models non-parsimonious, leading to more complexity and corresponding difficulty in optimization, yet the significant improvement in R^2 values derived from application of the ANN models on the three catchments offsets these weaknesses and justifies their application.

Table 4 Particulars of the network structure of the ANN models finally selected.

Station code no.	Neurons in the input layer		No. of neurons in the hidden layer	Total number of weights
	Total no.	Type of input series		
J2034010	9	nR:4, nE: , nS:1	3	34
J3024010	3	nR:2, nS:1	3	16
J4124420	5	nR:4, nS:1	5	36

nR, no. of rainfall data; nE, no. of evaporation data; nS, no. of outputs from SMARG.

The consensus simulation results, obtained by applying the MOCTs to the outputs of the individual substantive models in different combinations, are provided in Table 5 where it may be seen that the performance of the NNM is generally the best, followed by the WAM. The highest performance in calibration is generally achieved by the NNM combining outputs from all seven individual substantive models, although performance levels significantly higher than that of the best individual substantive model for any catchment could still be achieved by the NNM with less than seven combined outputs. SAM, being a special case of WAM, with equal weights, generally performs worse than the other two MOCTs.

Table 5 R^2 values in calibration (R_c^2) and verification (R_v^2) produced by MOCTs, and ranks.

Combinations for MOCTs		J2034010			J3024010			J4124420		
		R_c^2	R_v^2	Rank	R_c^2	R_v^2	Rank	R_c^2	R_v^2	Rank
All 7 models	SAM	84.27	81.55		84.68	73.62		87.37	83.87	
	WAM	94.05	92.14		92.73	88.62		93.55	94.24	
	NNM	96.00	86.27	1	93.51	83.54	2	94.86	90.59	1
Best 6	SAM	87.53	84.30		87.50	77.09		89.73	86.59	
	WAM	93.98	92.20		92.62	88.76		93.55	94.27	
	NNM	95.15	86.39	2	93.40	84.62	3	94.28	90.81	2
Best 5	SAM	90.73	87.26		89.20	79.19		91.57	89.28	
	WAM	92.51	91.23		92.00	88.11		93.41	93.64	
	NNM	93.41	85.89		93.53	84.77	1	94.19	88.30	3
Best 4	SAM	91.78	90.07		90.63	83.70		92.12	93.03	
	WAM	92.60	91.17		91.76	88.79		93.00	93.76	
	NNM	94.16	87.04	3	92.32	86.80		92.68	90.01	
Best 3	SAM	91.51	91.29		91.59	87.59		92.30	93.08	
	WAM	92.63	91.58		91.88	89.13		92.99	93.70	
	NNM	92.88	86.66		91.62	86.41		93.15	93.34	
Best 2	SAM	92.11	92.97		91.77	89.52		86.90	84.30	
	WAM	92.71	92.04		91.88	89.24		87.79	82.30	
	NNM	92.89	87.48		92.87	87.56		91.61	88.35	
% improvement of the best MOCT over the best individual model (of Table 3)		4.5			3.6			5.0		

For each of the three test catchments, the hydrographs of the rainfall, the observed discharge, and the discharge simulated by the best performing NNM model corresponding to the last water-year of the calibration period (i.e. the water-year at the middle of the data records used) are presented in Figs. 3, 4 and 5. It can be seen that the simulated discharge values in each case match fairly well with the corresponding observed discharges for that year, both in low as well as high flow values. The "time to peak" of the observed flows is also reproduced quite well.

CONCLUSIONS AND RECOMMENDATIONS

Amongst the individual substantive models, the performances of both forms of the naïve SLM (NP-SLM and P-SLM), which are very crude and simplified forms of the

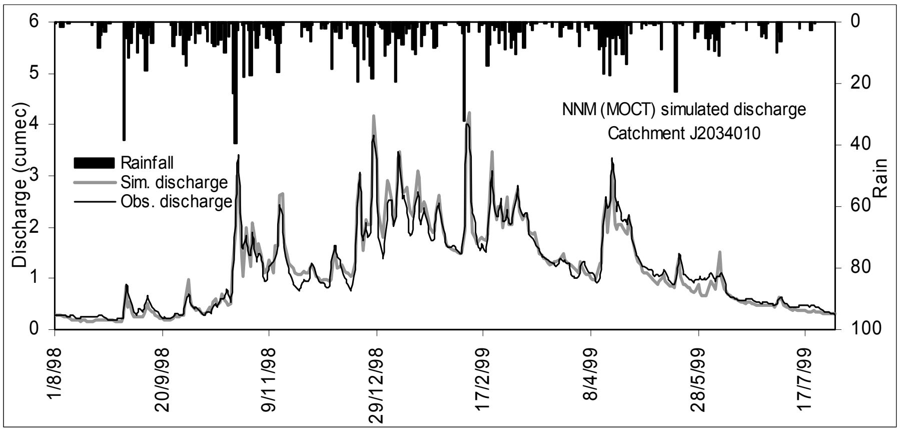

Fig. 3 Observed & simulated discharge and rainfall for the water year 1998–1999 for J2034010.

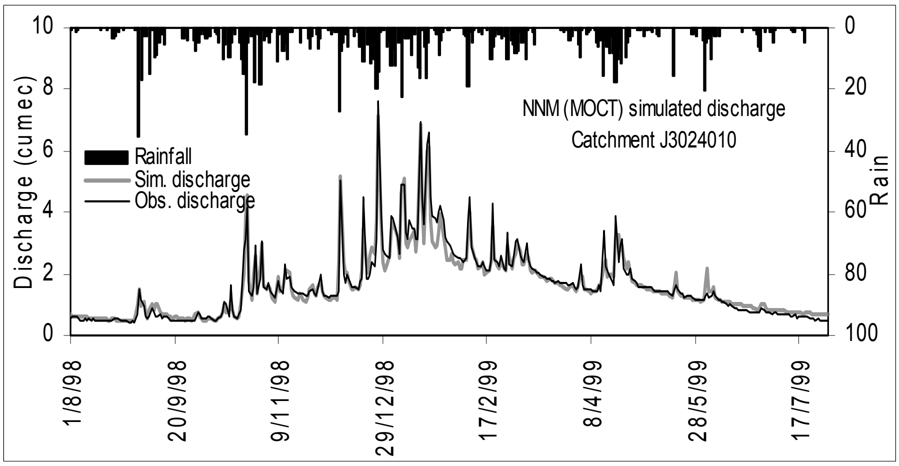

Fig. 4 Observed & simulated discharge and rainfall for the water year 1998–1999 for J3024010.

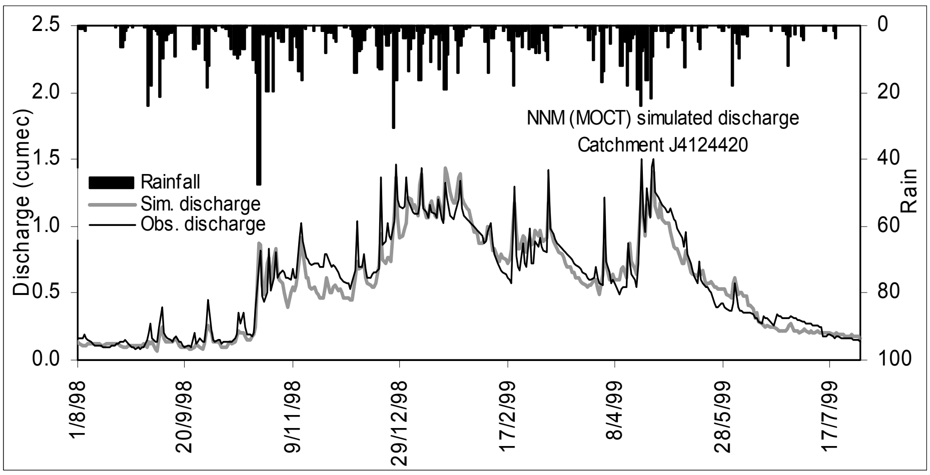

Fig. 5 Observed & simulated discharge and rainfall for the water year 1998–1999 for J4124420.

actual input–output transformation process, are found to be generally inferior to that of all other models tested. For these catchments, all characterized by substantial seasonality in the hydrological variables, both forms of the seasonally-based LPM (NP-LPM and P-LPM), significantly outperform the SLM model forms. For J4124420, the NP-LPM even outperforms the SMARG conceptual model. The SMARG conceptual model, which is intended to reflect the perceived dominant components of the physical process of flow generation in lumped form, generally performs better than the SLM and the LPM constructs. The performance of the wetness index based LVGFM, which utilizes SMARG as the auxiliary model for estimating the time-varying Gain Factor, is better than that of the SMARG, and hence better than the other four above-mentioned system-theoretic models. The ANN structure, however, despite being non-parsimonious, performs significantly better than all other models tested on the three catchments owing to its complex but flexible nonlinear formulation. Thus, the superiority of the ANN models over the conceptual and other system-theoretic types of rainfall–runoff transformation models on these catchments is established.

Outputs from all basic rainfall–runoff models, used in different combinations in MOCTs, are useful for obtaining the best consensus simulation of the observed flows whereby strengths of individual models are combined and perceptible weaknesses are discarded. In the case of the three test catchments, the simulated discharge obtained by such combination shows significant improvement, the performance of the NNM form of MOCT being the best.

Thus, among the MOCTs, the NNM is found to be the most efficient, establishing the overall superiority of the neural network topology in both parts of this study.

In future studies, it is planned to carry out tests to obtain lead-time flow forecasts of the flows, both with and without updating components, by developing and applying models that exploit recent mathematical tools such as wavelets, capable of emphasizing localized features, e.g. spikes for flash floods, etc. and the use of the NNM to combine radar precipitation estimates and raingauge data as inputs to semi-distributed catchment models.

REFERENCES

Ahsan, M. & O'Connor, K. M. (1994) A simple non-linear rainfall–runoff model with a variable gain factor. *J. Hydrol.* **155**, 151–183.

Birikundavyi, S., Labib, R., Trung, H. T. & Roussele, J. (2002) Performance of neural network in daily streamflow forecasting. *J. Hydrol. Engng ASCE* **7**(5), 393–398.

Campolo, M., Andreussi, P. & Soldati, A. (1999) River flood forecasting with a neural network model. *Water Resour. Res.* **35**(4), 1191–1197.

Dawson, C. W. & Wilby, R. (1998) An artificial neural network approach to rainfall–runoff modeling. *Hydrol. Sci. J.* **43**(1), 47–66.

Goswami, M, O'Connor, K. M. & Shamseldin, A. Y. (2002) Structures and performances of five rainfall–runoff models for continuous river-flow simulation. In: *Proc. 1st Biennial Meeting of Int. Env. Modeling and Software Soc.* (Lugano, Switzerland), **1**, 476–481.

Halff, A. H., Halff, H. M. & Azmoodeh, M. (1993) Predicting runoff from rainfall using neural networks. *Proc. Engng Hydrol., ASCE, NY* 760–765.

Hu, T. S., Lam, K. C. & Ng, S. T. (2001) River flow time series prediction with a range-dependent neural network. *Hydrol. Sci. J.* **46**(5), 729–745.

Jain, A. & Indurthy, S. K. V. P. (2003) Comparative analysis of event based rainfall–runoff modeling techniques-deterministic, statistical and artificial neural networks. *J. Hydrol. Engng* **8**, 93–98.

Kachroo, R. K. (1992) River Flow forecasting, Part 5 Applications of a conceptual model. *J. Hydrol.* **133**, 141–178.

Kachroo, R. K. & Liang, G. C. (1992) River flow forecasting. Part 2 Algebraic development of linear modelling techniques. *J. Hydrol*. **133**, 17–40.

Kachroo. R. K. & Natale, L. (1992) Non-linear Modelling of the rainfall–runoff relation. *J. Hydrol*. **135**, 341–369.

Minns, A. W. & Hall, M. J. (1996) Artificial neural neworks as rainfall–runoff models. *Hydrol. Sci. J.* **41**(3), 399–418.

Nash, J. E. & Sutcliffe, J. V. (1970) River flow forecasting through conceptual models. Part 1, A discussion of principles. *J. Hydrol*. **10**, 282–290.

O'Connor, K. M., Goswami, M. & Bhattarai, K. P. (2004) The Galway River Flow Modeling and Forecasting System (GFMFS) models. In: *4th MOPEX Workshop, CEMAGREF* (Workshop paper, in assoc. with NOAA, the USA), Paris, France.

Rajurkar, M. P., Kothyari, U. C. & Chaube, U. C. (2004) Modeling of the daily rainfall–runoff relationship with artificial neural network. *J. Hydrol*. **285**, 96–113.

Shamseldin, A. Y. (1997) Application of a neural network technique to rainfall–runoff modelling. *J. Hydrol*. **199**, 272–294.

Shamseldin, A. Y., O'Connor, K. M. & Liang, G. C. (1997) Methods for combining the outputs of different rainfall–runoff models. *J. Hydrol*. **197**, 203–229.

Shamseldin, A. Y. & O'Connor, K. M. (1999) A real-time combination method for the outputs of different rainfall–runoff models. *Hydrol. Sci. J.* **44**(6), 895–912.

Shamseldin, A. Y. & O'Connor, K. M. (2001) A non-linear neural network technique for updating of river flow forecasts. *Hydrol. Earth System Sci*. **5**(4), 577–597.

Sivakumar, B., Jawardena, A. W. & Fernando, T. M. K. G. (2002) River flow forecasting: use of phase-space reconstruction and artificial neural networks approaches. *J. Hydrol*. **265**, 225–245.

Smith, J. & Eli, R. N. (1995) Neural-network models of rainfall–runoff process. *J. Water Res. Plan. Manage. Div., ASCE* **121**(6), 499–508.

Tingsanchali, T. & Gautam, M. R. (2000) Application of tank, NAM, ARMA and neural network models to flood forecasting. *Hydrol. Proc*. **14**, 2437–2487.

Tokar, A. S. & Johnson, P. A. (1999) Rainfall–runoff modeling using artificial neural networks. *J. Hydrol. Engng, ASCE* **4**(3), 232–239.

Toth, E., Brath, A. & Montanari, A. (2000) Comparison of short-term rainfall prediction models for real-time flood forecasting. *J. Hydrol*. **239**, 132–147.

Zealand, C. M., Burn, D. H. & Simonovic, S. P. (1999) Short term streamflow forecasting using artificial neural networks. *J. Hydrol*. **214**, 32–48.